



**HAL**  
open science

## LES analysis of jets in cross flow

U. Bieder, P. Errante

► **To cite this version:**

U. Bieder, P. Errante. LES analysis of jets in cross flow. NUTHOS-11 - The 11th International Topical Meeting on Nuclear Reactor Thermal Hydraulics, Operation and Safety, Oct 2016, Gyeongju, South Korea. cea-02438721

**HAL Id: cea-02438721**

**<https://cea.hal.science/cea-02438721>**

Submitted on 28 Feb 2020

**HAL** is a multi-disciplinary open access archive for the deposit and dissemination of scientific research documents, whether they are published or not. The documents may come from teaching and research institutions in France or abroad, or from public or private research centers.

L'archive ouverte pluridisciplinaire **HAL**, est destinée au dépôt et à la diffusion de documents scientifiques de niveau recherche, publiés ou non, émanant des établissements d'enseignement et de recherche français ou étrangers, des laboratoires publics ou privés.

## LES analysis of jets in cross flow

**Errante P., Bieder U.\***

DEN-STMF, CEA, Université Paris-Saclay

F-91191 Gif-sur-Yvette ; France

Errante.Paolo@gmail.com

Ulrich.BIEDER@cea.fr

### ABSTRACT

Jets in cross flow are of fundamental industrial importance and play an important role in the validation of turbulence models. Two jet configurations are investigated with the TrioCFD code, the CFD reference code of the Nuclear Energy Division of CEA:

- A tee junction of circular tubes where a hot jet discharges into a cold main flow,
- A rectangular jet marked by a scalar discharging into a main flow in a rectangular channel.

The *tee-junction* configuration is very important for the phenomena of thermal fatigue. The OECD/NEA benchmark on the Vattenfall tee junction flow is analyzed. This test case is selected because, beside the experimental results, various calculation results with several turbulence modelling approaches have been published. A LES modelling and calculation strategy is developed and validated on this data for jets in crossflow under thermal fatigue conditions.

The *rectangular* jet configuration is important for basic physical understanding and modelling and has been analyzed experimentally at CEA. The experimental work was focused on the turbulent mixing between a rectangular channel flow with grid turbulence exiting a heated jet into a confined grid turbulent crossflow, with both kinematic and passive scalar high quality measurements in order to characterize its statistical properties (energy spectra, Reynolds stresses (anisotropy), PdF). These experiments are analyzed for the first time with LES by applying the strategy developed for the Vattenfall configuration. The turbulent inlet boundary conditions are well controlled in both experiment and calculation (grid turbulence). Structured and unstructured tetrahedral grids are used to predict the measured mean values and turbulent fluctuations of the velocity and the temperature.

### KEYWORDS

**LES, jet, cross flow, turbulence**

## 1 INTRODUCTION

During the last decades, thermal fatigue issues have been observed in beside zones where two fluids at different temperature are mixed. Temperature fluctuations driven by turbulent flows induces thermal stress cycles on piping's material and can provoke crack initiation with a consecutive structural wreckage if not detected in time. Several failures have been observed in nuclear reactor's coolant mixing junctions, most of them located aside safety injection lines and steam generator feed water nozzles as well as surge line nozzles and pipes. Normally, the damaged parts shows the presence of wall crack penetrations along geometrical or structural singularities as elbows or weldings.

The most significant thermohydraulic parameters which plays an important role on the formation and the consequent progression of these structural insufficiencies, are related to the thermal gradient and its time derivative, so often temperature differences between streams ( $\Delta T$ ), frequencies ( $\omega$ ) and number of cycles ( $N$ ) are convenient variables to be used on the thermal fatigue analysis.

A really great number of experimental campaigns<sup>1</sup> have been conducted upon this subject and the outcomes demonstrated that, typically, thermal loads characterized by  $\Delta T$  of about 160 K and  $\omega$  between 3 and 10 Hz, seems to create favorable conditions to crack initiations. Beside the aim of providing the critical intervals of this parameters, experimental data have been also produced to validate Computational Fluid Dynamics (CFD) codes and further model's developments. In fact, due to correctly predict and avoid thermal striping problems, CFD tools shows an interesting potential and its application can lead to an in-depth comprehension upon complex operating conditions and geometries which are difficult and/or expensive to be reproduced for empirical investigations.

In a large part of cases, turbulent flows can be described with good accuracy and small computational costs by using two-equation models for solving Reynolds Averaged Navier-Stokes Equations (RANS) whenever the user aims to obtain consistent time-averaged fields. On the other hand, for obtaining reasonable values in terms of local time fluctuations, Large Eddy Simulation (LES) shows higher potentials with better capabilities, despite its greater computational costs, on catching the desired parameters for thermal fatigue analysis. However, detailed validations on CFD codes are still needed to achieve a better comprehension on their limits whenever they're used for studying such kind of phenomenon. In the present paper, two experimental campaigns are taken in account as a measuring tape for evaluate the *TrioCFD* code developed in the Saclay research center of CEA.

## 2 SETUP OF THE ANALYSED EXPERIMENTS

A big experimental and numerical effort is needed to achieve a good agreement between experimental and CFD data and to verify the reliability of CFD codes for thermal fatigue analysis. The experimental data used for the validation of the *TrioCFD* code are originated from:

- T-junction mixing tests carried out at the Alvkärlaby Laboratory of Vattenfall Research and Development in Sweden during November 2008 [1], proposed to test the ability of state-of-the-art of CFD codes to predict the important parameters affecting high cycle thermal fatigue in mixing tees. The main aim of this project is basically to give reference results for CFD benchmarks, but also to allow the scientific community to compare the outcomes given by different numerical approaches;
- TRANSAT closed-loop wind tunnel of the CEA center located in Grenoble [2]. Several experiences have been done to study the thermal-fluid-dynamics properties of cross-flow jet interactions, varying the ratios between the jet and the main stream velocity  $r = \frac{U_j}{U_\infty}$  to give a valid reference for rectangular section's ducts and a closer view to the interactions between the jet flow and the opposite wall for higher values of  $r$ . This experimental campaign had also the objective to satisfy the request of non-academically reference cases for the *TrioCFD* code validations. The physical phenomenon involved in the experiments are characterized by transient and 3D vortices structures, which provides a formidable challenge from a numerical point of view.

Focusing on the turbulent mixing of jets, the main parameters of interests are often reported in adimensional form. Since the main phenomenons are driven by temperature and velocity gradients, the absolute values aren't intimately representative, thus, all the information can be condensed in non-dimensional form in order to easily evaluate where the mixing phenomenons are pronounced and,

---

<sup>1</sup>One can refer to the SPLASH, FATHER, AIRJECO and NAJECO investigations

moreover, they allows potential comparisons between different operative conditions. Here below are listed the definitions of the common main parameters observed to characterize thermal loads and their relationship with the velocity field:

- Time Average, root mean square and Fourier transform of the general scalar  $\phi$ :

$$\bar{\phi} = \frac{1}{\Delta t} \int_t^{t+\Delta t} \phi(t) dt; \quad \sigma_\phi = \sqrt{\frac{1}{\Delta t} \int_t^{t+\Delta t} (\phi(t) - \bar{\phi})^2 dt}; \quad \tilde{\phi}(\omega) = \int_{-\infty}^{\infty} \phi(t) e^{-2\pi i t \omega} dt; \quad (1)$$

- The non-dimensional temperature and non-dimensional amplitude of the fluid temperature fluctuations.

$$T^* = \frac{T - T_{cold}}{T_{hot} - T_{cold}}; \quad \sigma_T^* = \frac{\sigma_T}{T_{hot} - T_{cold}} \quad (2)$$

- The non-adimensional velocity i-component and non-dimensional amplitude of the velocity i-component fluctuations:

$$u_i^* = \frac{u_i}{U_{bulk}}; \quad \sigma_{u_i}^* = \frac{\sigma_{u_i}}{U_{bulk}} \quad (3)$$

## 2.1 The Vattenfall T-Junction experiment

The experimental section consists in two manufactured Plexiglas tubes connected by a hollowed cube to form a T-shape. The first pipe, horizontally positioned, has an inner diameter ( $D_2$ ) of 140 mm and transports a 9 l/s ( $Q_2$ ) water flow at the temperature of 292 K, while the branch pipe with a diameter ( $D_1$ ) of 100 mm transports a water flow ( $Q_1$ ) of 6 l/s at the temperature of 309 K. All the structures have been disposed for reducing as much as possible heat losses. Temperature's fluctuations were measured with a frequency of 200 Hz for 300 s using thermocouples placed 1 mm from the pipe walls along the circumference of the inner pipe at angles of  $0^\circ$ ,  $90^\circ$ ,  $180^\circ$ ,  $270^\circ$ . All the thermocouples are located downstream of the tee junction at distances of two, four, six and eight hydraulic diameters. Two additional thermocouples were placed at angular locations of  $0^\circ$  and  $180^\circ$  downstream at fifteen and twenty hydraulic diameters. The measurements were given in form of mean, RMS and turbulence statistics values.

Velocity profiles were measured at 1.6, 2.6, 3.6 and 4.6 hydraulic diameters downstream of the tee junction using a two component LDV system. Time averaged and RMS fluctuations were provided for the x ( $U$ ) and z ( $W$ ) velocity components along the vertical diameter line at each of the four locations. For the x and y ( $V$ ) velocity components, analogous data are given on the horizontal diameter line. PIV data was collected at frequency of 60 Hz for 12 s. Supplementary details on measurements points are described in Fig.1.

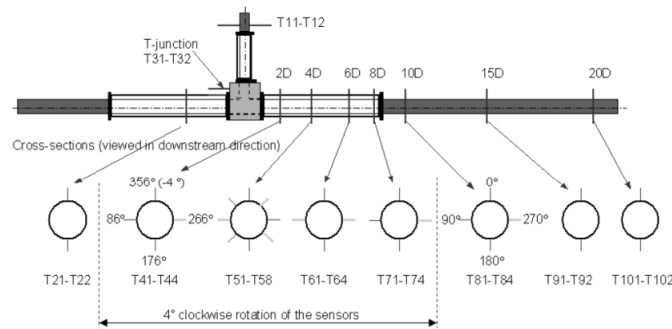


Figure 1: Schematic sketch of the Vattenfall tee junction test section

## 2.2 The TRANSAT experiment

The TRANSAT facility is a closed loop wind-tunnel located at CEA Grenoble. A simplified scheme of the overall structure of the tunnel is showed in Fig.2.

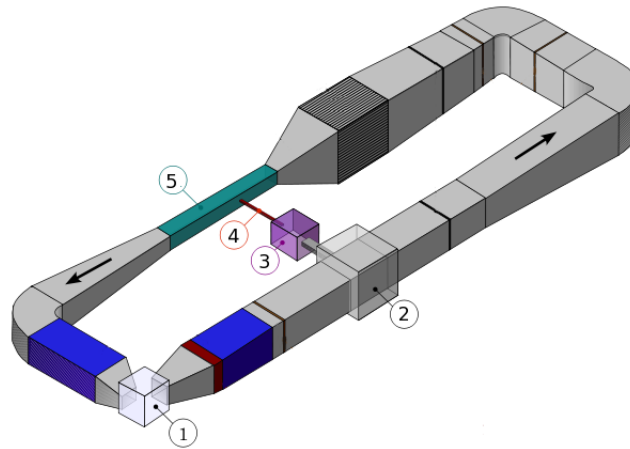


Figure 2: Schematization of the TRANSAT wind-tunnel sections

Following the index numbers in Fig 2, TRANSAT consists of:

1. A centrifugal fan which can give a maximum flowrate of  $4.5 \text{ m}^3 \cdot \text{s}^{-1}$  using an electrical synchronous 8 kW engine controlled with an inverter.
2. A jet collector, where a part of the main channel air flow is collected to feed the jet.
3. An adjustable heater which heats up the jet flow with 0 to 5 thermal kW.
4. The Jet channel which contains a sequence of silencer, calm chamber and convergent ducts, analogously to the main channel. It has a total length of 3 m and an outlet rectangular section 50 mm high ( $H_j$ ) and 80 mm width ( $L_j$ )
5. The test section located at the outlet of the convergent duct, has a rectangular section 0.6 m width ( $L_c$ ) and 0.5 m high ( $H_c$ ) for a length of 5 m. The jet channel outlet is situated at middle height, 2.1 m downstream from the main channel inlet section (Fig.3).

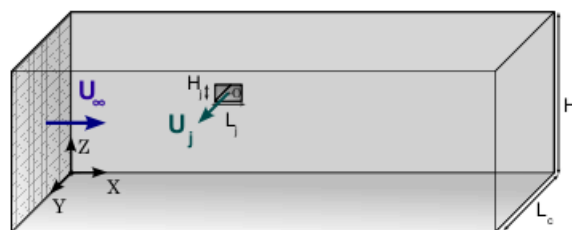


Figure 3: Schematic sketch of the TRANSAT test section

The whole length of the wind tunnel is coated to keep the main air flow temperature between 286 and 288 K and attenuate environment effects. The jet heater is calibrated to give a  $\Delta T$  of 10 K.

In order to find an optimal basic setup, the CFD calculation is focused on those experimental conditions in which the interactions between the jet and the wall can be assumed negligible. This configuration is characterized by an  $r$  ratio of 3.3 where the jet bulk speed ( $U_j$ ) is  $7 \text{ m.s}^{-1}$  and the main channel bulk speed ( $U_\infty$ ) is  $2.1 \text{ m.s}^{-1}$ .

Measurement of velocity components were taken using several hotwire anemometers with a sample frequency of 21 kHz. The instruments are located on planes parallel to the main channel section at 240, 480 and 680 mm downstream of the jet inlet, others are parallel to the jet section located at 2 and 20 mm away from the jet outlet. Moreover, temperature has been investigated in a plane perpendicular to the previous two planes, placed at the middle height of the channel. At the same positions of the hotwire anemometers, Pt 100 RTD's have been used to take temperature measurements with frequencies up to 50 kHz. Temperature data are given in terms of averaged non-dimensional values as expressed in Eq.(2).

### 3 THE BASIC EQUATIONS OF THE CFD MODEL

The *TrioCFD* code has been used to perform calculations on both experimental test cases. Preemptive simulations have been carried out using unsteady RANS equations with  $k - \varepsilon$  model, in order to achieve a better understanding on the grid refinement and the accuracy on both boundaries and initial conditions. All this information is strictly needed to correctly setup the large eddy simulation. The  $k - \varepsilon$  model also helps to evaluate whereas it's a reasonable choice to reduce the domains size, allowing less costs in terms of memory and CPU time spent. This gives the possibility to tests a higher number of different setups in a short-time. Hereafter LES calculations have been performed to make a final comparison with the experimental datas provided.

The *TrioCFD* code is designed for both incompressible and low Mach number compressible single phase flows. The work related to this article treats the first assumption, since the experimental conditions doesn't present important density gradients. Moreover, the Richardson number doesn't exceed a scale of  $10^{-2}$ , hence convective effects overtake buoyancy and its associated term (Boussinesq approximation) is neglected. Thermal sources are absent, so its relative term is not considered as well while the deviatoric part of the Cauchy tensor follows the Newtonian fluid hypothesis. The turbulent contributions terms employs the Boussinesq hypothesis. Here is given the set of partial differential equation used in this study:

$$\nabla \cdot \vec{u} = 0 \quad (4)$$

$$\frac{\partial \vec{u}}{\partial t} + \vec{u} \cdot \nabla \vec{u} = -\nabla \left( \frac{p}{\rho} \right) + \nabla \cdot ((\nu + \nu_t)(\nabla \vec{u} + \nabla^T \vec{u} - \frac{2}{3} \nabla \vec{u} I) + \vec{g}) \quad (5)$$

$$\frac{\partial T}{\partial t} + \vec{u} \cdot \nabla T = \nabla \cdot ((\alpha + \alpha_t) \nabla T) \quad (6)$$

In the following sections details about the two tested turbulence models are discussed.

#### 3.1 RANS $k - \varepsilon$ model

In the RANS approach, Reynolds averaging is applied on the instantaneous turbulent quantities. In combination with the eddy viscosity concept of Boussinesq, this leads formally to eq.s 4, 5 and 6 where the unknowns represent time averaged values. The  $k - \varepsilon$  model links the turbulent viscosity ( $\nu_t$ ) directly to the turbulent kinetic energy ( $k$ ) and its dissipation rate ( $\varepsilon$ ) and assuming the similarity of

turbulent heat and mass transfer, the turbulent thermal diffusivity ( $\alpha_t$ ) is calculated from the turbulent Prandtl number ( $Pr_t$ ):

$$\nu_t = C_\mu \frac{k^2}{\varepsilon}; \quad \alpha_t = \frac{\nu_t}{Pr_t} \quad (7)$$

Conservation equation are given then for both  $k$  and  $\varepsilon$  :

$$\frac{\partial k}{\partial t} + \vec{u} \cdot \nabla k = \nabla \cdot \left( \frac{\nu_t}{\sigma_k} \nabla k \right) - \varepsilon + P \quad (8)$$

$$\frac{\partial \varepsilon}{\partial t} + \vec{u} \cdot \nabla \varepsilon = \nabla \cdot \left( \frac{\nu_t}{\sigma_\varepsilon} \nabla \varepsilon \right) - C_{\varepsilon 2} \frac{\varepsilon^2}{k} + C_{\varepsilon 1} P \frac{\varepsilon}{k} \quad (9)$$

Where the production of turbulent kinetic energy ( $P$ ) is written as:

$$P = -\overline{u'_i u'_j} \frac{\partial \bar{u}_i}{\partial x_j}; \quad \overline{u'_i u'_j} = \frac{2}{3} k \delta_{ij} - \nu_t \left( \frac{\partial \bar{u}_i}{\partial x_j} + \frac{\partial \bar{u}_j}{\partial x_i} \right) \quad (10)$$

Details about the standard values of constants are reported in the following Table 1:

**Table 1. Transport equation constants**

$C_\mu$	$\sigma_k$	$\sigma_\varepsilon$	$C_{\varepsilon 1}$	$C_{\varepsilon 2}$	$Pr_t$
0.09	1.0	1.3	1.44	1.92	0.9

### 3.2 LES WALE model

In the LES approach, a filtering operation is applied on the instantaneous turbulent quantities. In combination with the eddy viscosity concept of Boussinesq, this leads formally to eq.s 4, 5 and 6 where the unknowns represent filtered values. With the aim to better reproduce the transition from laminar to turbulent flow and to obtain a correct wall-asymptotic-behavior of the turbulent viscosity, the Wall Adaptive Local Eddy-viscosity (WALE) model [3] has been developed. This model offers all the advantages of the Dynamic Smagorinsky model without requiring explicit filtering operations. The turbulent viscosity of the WALE model respond to the following equations:

$$\nu_t = \Delta_s^2 \frac{(S_{ij}^d S_{ij}^d)^{\frac{3}{2}}}{(\bar{S}_{ij} \bar{S}_{ij})^{\frac{5}{2}} + (S_{ij}^d S_{ij}^d)^{\frac{5}{4}} + 10^{-6}}; \quad (11)$$

$$\bar{g}_{ij} = \frac{\partial \bar{u}_i}{\partial x_j}; \quad \Delta_s = C_w V^{\frac{1}{3}}; \quad (12)$$

$$\bar{S}_{ij} = \frac{1}{2}(\bar{g}_{ij} + \bar{g}_{ji}); \quad S_{ij}^d = \frac{1}{2}(\bar{g}_{ij}^2 + \bar{g}_{ji}^2) - \frac{1}{3} \delta_{ij} \bar{g}_{kk}^2; \quad (13)$$

The  $C_w$  coefficient is set to be 0.5

## 4 SETUP OF THE NUMERICAL MODELS

The calculations domains have been discretized using tetrahedral elements, in both structured and unstructured forms. *TrioCFD* use a finite volume based finite element (VEF) approach to integrate in conservative form all the balance equation over the control volumes belonging to the domain. As in the classical Crouzeix–Raviart element, both vector and scalar quantities are located in the center of the faces. The pressure however is discretized around the vertices and the volume's center of gravity as shown in [6] for the 2D case. This discretization leads to a very good pressure/velocity coupling and has a very dense convergence free basis. Along this staggered mesh structure, the unknowns, i.e. vector and scalar values, are expressed using non-conforming linear shape-functions (P1-non-conforming). The shape function for the pressure is constant for the center of the element (P0) and linear for the vertices (P1).

For RANS calculations, the first order Euler backward implicit schemes is used for the time discretization and a MUSCL type convection scheme is selected. The implicit scheme ensures good stability of the steady state solution. The higher computational cost required per iteration is compensated by a lower number of elements generally needed in the calculation domain to achieve a good approximation of the fields. For LES calculations, the second order Adams-Bashforth scheme is used and a slightly stabilized second order centered convection scheme is selected. For the simulation of unsteady flows using LES, a finer spatial grid is required to account for the effects related to sub-grid scale modeling. Therefore, implicit methods are usually not suitable for LES. The time discretization should adopt its accuracy dependently on the refinement of the spatial discretization. Hence, only explicit (multi-step) methods are suitable for LES calculations.

The discretized momentum balance equations are solved following the SOLA pressure projection method of Hirt et al. [7]. The resulting Poisson equation is solved with a conjugate gradient method using a symmetric successive over relaxation technique to improve convergence. The convergence threshold has been set to  $10^{-6}$  for all calculations presented here.

The presented CFD calculations have been carried out exploiting the code's parallelization capabilities. Each domain is decomposed into several overlapping sub-domains thanks to METIS libraries; all sub-domains were equally distributed among different processor cores which communicate mutually only when data transfer is necessary by using message passing interface libraries (MPI).

### 4.1 Vattenfall T-Junction

Since velocity profiles are given at 3.1 hydraulic diameters upstream of the junction for the main pipe and 3 hydraulic diameters for the branch pipe, the overall calculation domain has been shortened upstream to this extent. This shortened domain is in accordance to most of the previous works (i.e. Höhne [4] and Frank et al. [5]). The upstream profiles, described in detail by Smith [1], are assumed constant in time and space and being axisymmetric. The interpolation made on the original data reproduce the original flow rates with an error of 1 %. For the  $k - \varepsilon$  model, the turbulent kinetic energy has been taken coherently with the root mean square values given by Smith [1].

For the LES approach, Kuczaj [8], Odemark [9] and Westin [10] independently proved that the inlet turbulence's level is not considered as a relevant element for final results. In fact, since the main turbulence's generation relies on the mixing zone, inlet turbulence profiles don't play an important role in the overall flow behavior. Therefore, the inflow profiles have been taken constants with time. An uniform zero static pressure field has been set on the outlet section and Reichardt's wall function [11] described in eq.(14) has been applied on the pipe's boundary walls. The water physical properties have been taken from Perry's Chemical Engineers' Handbook.

$$u^+ = \frac{1}{\kappa} \ln(1 + \kappa y^+) + 7.8 \left[ 1 - \exp\left(-\frac{y^+}{11}\right) - \frac{y^+}{11} \exp\left(-\frac{1}{3}y^+\right) \right] \quad (14)$$

The time required to approach a fully developed turbulent flow in the whole domain doesn't overtake in average more than five seconds. Monitoring points have been defined on corresponding locations described by the experimenters for comparison with data. The duration to collect statistics last not less than 10 s.

Unstructured, structured and hybrid meshes composed by tetrahedrons have been created aiming to obtain a mesh independency on results. Three examples are reported in Fig. 4. Mesh refinement tests have been performed starting from 0.8 million up to 9 million grid elements in the domain. The averaged  $y^+$  values calculated on the walls vary from 7.48 to 0.72 passing from the coarser mesh to the finest one. Elements' largest angles are between  $60^\circ$  and  $100^\circ$ .

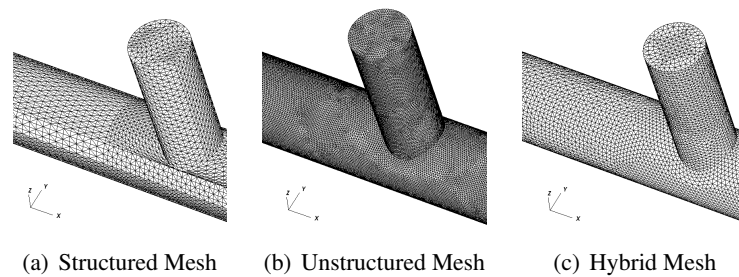


Figure 4: Mesh examples

## 4.2 TRANSAT

Preliminary  $k - \varepsilon$  calculations were performed to analyze the effect of reducing the domain upwind of the jet outlet. Due to this analysis, the test section has been finally shortened to 0.4 m upstream and 1.2 m downstream the jet outlet section. The experimental facility has especially been designed to obtain homogeneous characteristics in terms of turbulence and velocity profiles close to the inlets sections. Thus, flat velocity profiles have been used as boundaries conditions for both main ( $2.1 \text{ m} \cdot \text{s}^{-1}$ ) and jet channel ( $7 \text{ m} \cdot \text{s}^{-1}$ ).

Following the same considerations given in the previous section, turbulence inlet levels have not been taken in account for LES as a value of only 1% has been measured at these locations for the turbulence intensity [2]. At the outlet section, a zero static pressure has been set and Reichardt's wall-function (eq.(14)) has been applied to the solid walls. The flow time needed to stabilize the fluctuating fields is about five seconds, afterwards statistics were collected for the following 14 seconds on the measuring plans described in section 2.2.

Concerning the domain discretization, 1 million to 18 million mesh elements have been used during the work, producing  $y^+$  values between 2.39 and 27.9 with minimum mesh angles of 35 degrees. Both time and space discretization schemes already used for the Vattenfall case have been used for the TRANSAT simulations.

## 5 RESULTS

### 5.1 Vattenfall T-Junction

The most representative comparisons between experiment and calculations are shown. Fig. 5 shows horizontal, vertical and axial profiles of the mean and RMS values of both velocity and temperature at different locations downstream of the junction (locations see Fig.1).

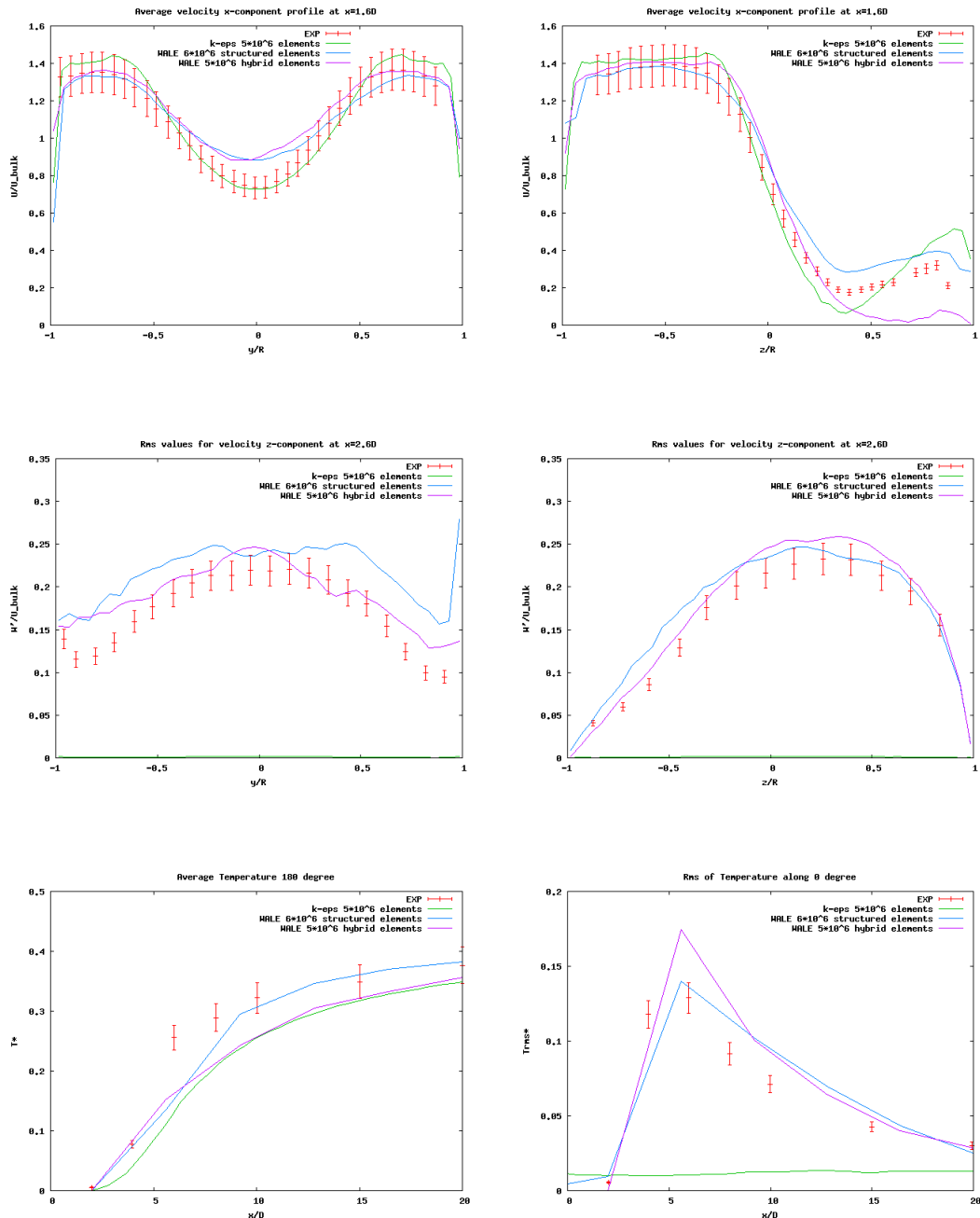


Figure 5: Comparison between experiments and CFD data

RANS and LES calculations are compared to the experimental values. As already underlined in the introduction, the  $k-\epsilon$  model produce adequate results in terms of average profiles, but the structure of RANS equation doesn't allow to obtain meaningful information on temporal fluctuations. However, the LES model is able to catch coherently the behavior of both average and RMS profiles.

In Fig 6 a comparison between LES (left) and experiment (right) is illustrated for discrete Fourier Transforms of temperature, located two hydraulic diameters downstream the junction. The LES spectrum (hybride meshing with 5 million elements) reproduces the fluctuations amplitudes for lower frequencies, thereafter the slope starts to follow correctly a  $-5/3$  law. However, the main shedding frequency detected in the experimental data at 3 to 5 Hz is not reproduced in the LES for this location. Further analysis is needed to understand this discrepancy.

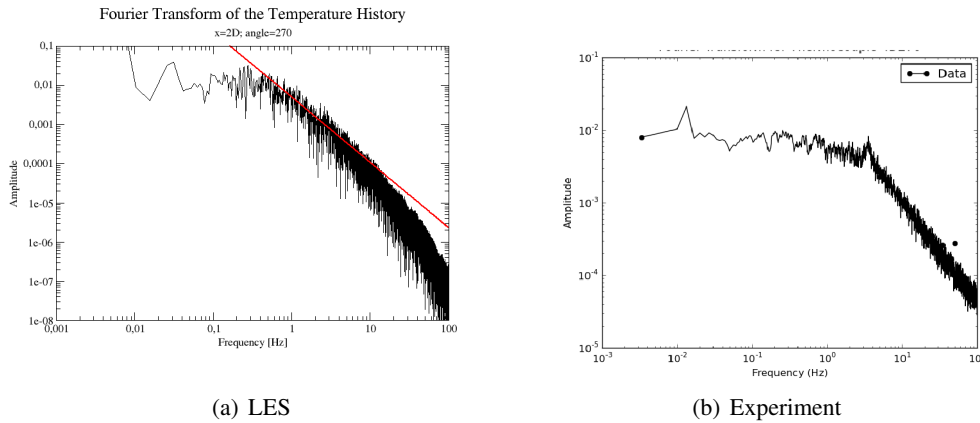
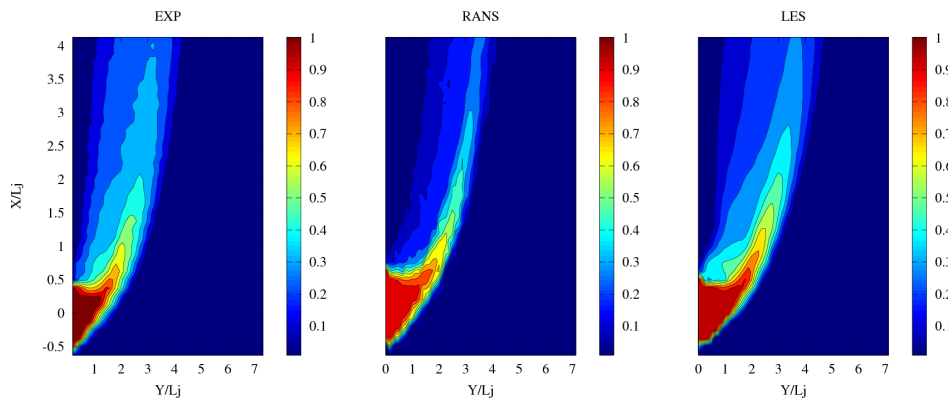


Figure 6: Comparison between Temperature spectras

## 5.2 TRANSAT

As for the Vattenfall T-Junction, comparison between TRANSAT experiments and CFD results are shown in form of temperature average and RMS values. Closer agreement with the experimental data are achieved progressively with the mesh refinement. This is true for both, RANS and LES. In terms of mean values, coarser meshes allow to obtain reasonable predictions. However, to capture the observed turbulent statistics of the scalars, finer meshes improve the LES outcomes. It is important to note that finer meshes give not only a better resolution of the turbulent behavior at high frequencies but also at the scales of interest, which are in this case, the temperature fluctuations between 0.1 and 10 Hz.

Fig. 7 shows temperature mean and RMS values in a horizontal cut plane in the center of the channel (see Fig.3). Experimental values are compared to RANS and LES results. The same considerations already made for the comparisons between  $k - \varepsilon$  and WALE models can be done; RANS can reproduce correctly the averages values but does not allow access to any correct information on the fluctuating quantities.



(a) Time-Averaged non-dimensional Temperature

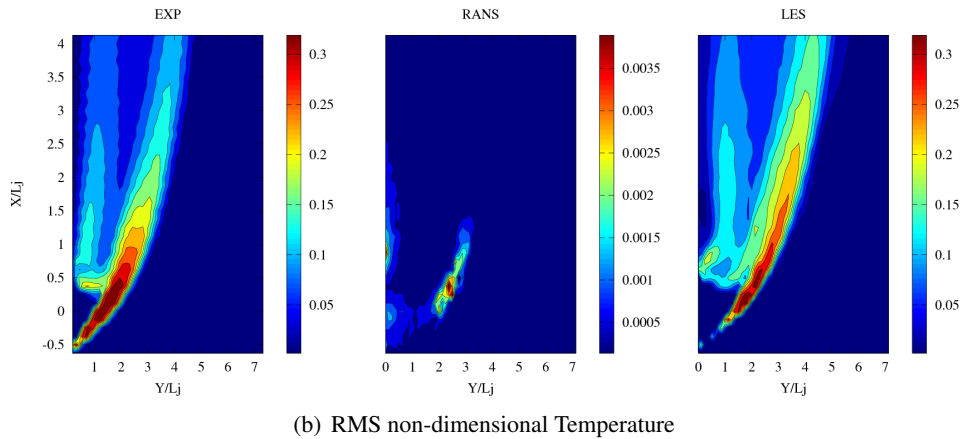


Figure 7: Plane  $xy$ ;  $z = 0$  mm, from left to right experimental data,  $k - \varepsilon$  and WALE results

Figures 8 show temperature mean and RMS values close to the jet outlet in a vertical cut plane 20 mm from the channel wall. The temperature fluctuations near the impact zone between jet and main flow is under-predicted by the LES calculation, especially on the extra-dos of the jet. It seems that the boundary layers in the jet inlet channel are not correctly resolved since the wall law still has an influence in this zone ( $y^+ = 10$ ).

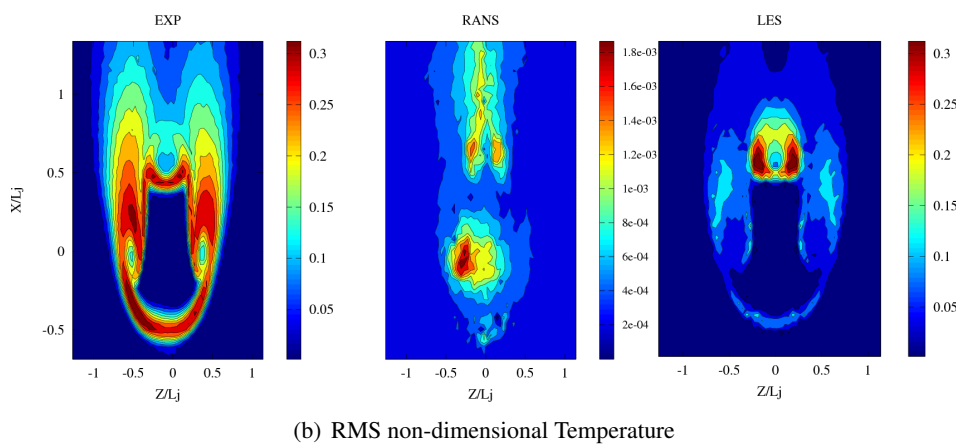
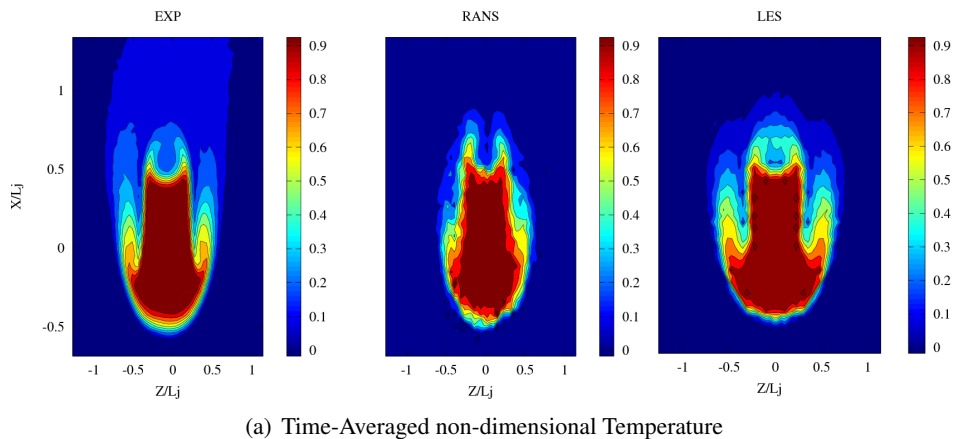


Figure 8: Plane  $xz$ ;  $y = 20$  mm, from left to right experimental data,  $k - \varepsilon$  and WALE results

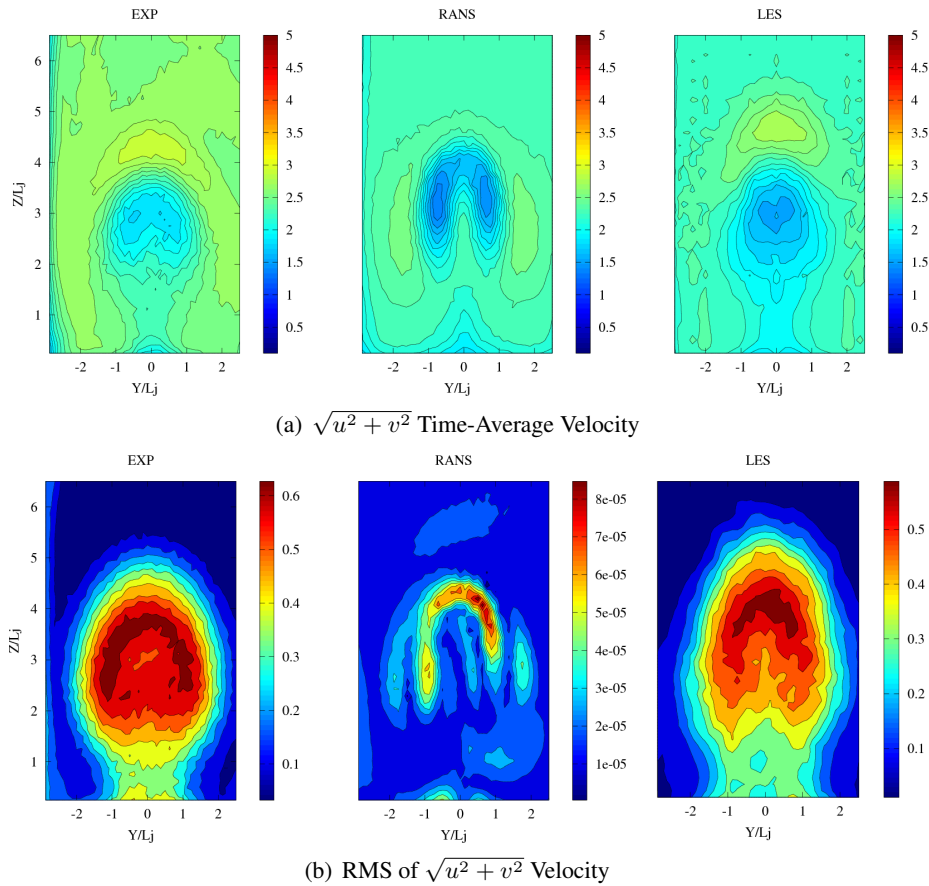


Figure 9: Plane  $yz$  at  $x = 480$  mm, from left to right experimental data,  $k - \varepsilon$  and LES results

The turbulent fluctuations are better predicted in zones where the jet penetration depth reach higher distances from the main channel walls. This can be seen from Fig. 9 where time averaged and RMS values of the velocity are given in vertical cut planes normal to the main channel walls. The axial distance of the plane from the jet outlet is 480 mm (see Fig.3).

## 6 CONCLUSION

Mixing phenomenon involved in jets in crossflow configurations still represent a challenge for CFD applications. The appropriate resolving of small scales required for the correct modeling of the transient behavior of highly turbulent flows represent one of the most important parameters with respect to the quality of the results. The comparisons performed on the Vattenfall and TRANSAT test cases have shown encouraging responses of CFD, especially for LES. The progressive increase of computer power will allow to capture more and more details of the turbulence and thus allow to approach the needed time and spatial discretization scales.

## 7 ACKNOWLEDGEMENT

This work was granted access to the HPC resources of CINES under the allocation x2016a7571 made by GENCI.

## References

- [1] Brian Smith, et al., July 2009. OECD/NEA VATTENFALL T junction benchmark specifications. OECD/NEA Report.
- [2] Pierre Fougairolle, July 2009. Caractérisation expérimentale thermo-aéraulique d'un jet transverse impactant ou non, en turbulence de conduite. CEA Grenoble Thèse.
- [3] Nicoud, F., Ducros, F., 1999. Subgrid-scale modelling based on the square of the velocity gradient tensor. *Flow Turbul. Combust.* 62, 183–200.
- [4] Höhne T., 2014. Scale resolved simulations of the OECD/NEA-Vattenfall T-Junction benchmark. *Nuclear Engineering and Design.* 269, 149–154.
- [5] Frank T. et al., 2008, Simulation of Turbulent and Thermal Mixing in T-Junctions Using URANS and Scale-Resolving Turbulence Models in ANSYS-CFX, XCFD4NDRS. Grenoble, France, Paper MIX, 07.
- [6] Höhne T., Kliem S. Bieder U., 2006, Modelling of Bouyancy driven flow experiment at the RO-COM test facility using the CFD codes CFX-5 and Trio-U, *Nuclear Engineering and Design*, 236, 12, 1309–1325
- [7] Hirt, C.V., Nichols, B.D., Romero, N.C., 1975. SOLA—a numerical solution algorithm for transient flow. Los Alamos National Lab., Report LA-5852.
- [8] Kuczaj, A. K., de Jager, B., Komen, E. M. J., 2008. An assessment of large eddy simulation for thermal fatigue prediction. *International Congress on Advances in Nuclear Power Plants.*
- [9] Odemark, Y., Green, T. M., Angele, K., Westin, J., Alavyoon, F., Lundstrom, S., 2009. High-cycle thermal fatigue in mixing tees: new LES validated against new data obtained by piv in the vattenfall experiments. *ICONE-17.*
- [10] Westin, J., Mannetje, C., Alavyoon, F., Veber, P., Andersson, L., Andersson, U., Eriksson, J., Henriksson, M., Andersson, C., 2008. High-cycle thermal fatigue in mixing tees. large eddy simulations compared to a new validation experiment. *ICONE-16.*
- [11] Hinze J.O., 1959, *Turbulence*, McGraw-Hill